Internal Rotation of the CF_3 Group in the (Trifluoromethyl)anilines: A Zero-Kinetic-Energy Pulsed-Field-Ionization Study†

Neil A. Macleod

Physical and Theoretical Chemistry Laboratory, University of Oxford, South Parks Road, Oxford OX1 3QZ, U.K.

Kenneth P. Lawley* and Robert J. Donovan

Department of Chemistry, University of Edinburgh, West Mains Road, Edinburgh EH9 3JJ, Scotland

Received: October 31, 2000; In Final Form: February 6, 2001

Internal rotation in the ionic ground states of 1-, 2-, and 3-(trifluoromethyl)aniline (ABTF) have been studied by high-resolution photoelectron spectroscopy (ZEKE-PFI) using the S_1 state as the resonant intermediate. Coefficients of the torsional potential of the CF_3 group obtained from a one-dimensional rigid rotor model were as follows: 2-ABTF, V_3=720 ± 10 cm^{-1}, $V_6 = -3 \pm 3$ cm^{-1}; 3-ABTF, $V_3 = 222 \pm 10$ cm^{-1}, $V_6 = -4 \pm 2$ cm^{-1}; and 4-ABTF, $V_6 = 12 \pm 5$ cm^{-1}, with little change in the rotational constant of the rotor. These values display trends consistent with those found for the CH_3 rotor in the same environment. In particular, the equilibrium conformation of the rotor changes on ionization from the S_1 state by 60° in the 3-isomer, but is unchanged in the 2- and 4-isomers. Symmetry forbidden transitions, leading to marked non-Franck−Condon behavior of intensities in the ZEKE spectra of the meta isomer are observed to be far more extensive than in the corresponding CH_3 case. A further factor directly affecting the ZEKE spectrum in the ortho isomer is the coupling between the adjacent CF_3 and NH_2 rotors, which is far more pronounced than with CH_3 and NH_2.

1. Introduction

A number of zero electron kinetic energy (ZEKE) studies[1] have been reported on a range of substituted toluenes from which the potential energy function for internal rotation of the methyl group in the ion can be deduced. Each of the three geometric isomers of a monosubstituted toluene displays a unique dependence of the barrier height for internal rotation on the electronic state.[2] The para or 4-isomers[3] display only a small 6-fold barrier of less than 50 cm^{-1} in the S_0, S_1, and ionic D_0 states, similar to toluene itself.[4] In contrast, the meta or 3-isomers have 3-fold barriers which are negligible in S_0, but which increase dramatically on excitation to the S_1 state, and the whole potential then shifts by 60° on ionization. The ortho or 2-isomers behave in the opposite manner. A large barrier, ≥300 cm^{-1}, in the S_0 state is reduced to less than 50 cm^{-1} in the S_1 state but returns to its previous high value in the ion. The equilibrium conformation of the rotor changes by 60° on $S_1 \leftarrow S_0$ excitation in the halotoluenes and then changes back in the ion. In 2-aminotoluene, however, the equilibrium conformations remain the same in all three electronic states.

Several explanations for this varied behavior have been suggested. Simple steric changes in the rotor are not responsible because no significant correlation in the rotational constant $\tilde{F}$ has been found; for example in 2-aminotoluene, $\tilde{F} = 5.28$, 5.40, and 5.20 cm^{-1} in the S_0, S_1, and D_0 states, respectively.[5] Weisshaar and co-workers[2], through ab initio calculations on the ground state and ion, have found a significant correlation between the geometry of the benzene ring close to the rotor and the barrier/conformation of the potential for internal rotation. Similar conclusions can be reached by consideration of individual resonance structures to the wave function that involve hyperconjugation between the molecular orbitals of the ring and rotor. Recently, Nakai and Kawai[6] have examined the effects of hyperconjugation between the empty π^* antibonding orbital of the rotor and the aromatic π-system. They found striking differences between the HOMO and LUMO orbitals for both ortho and meta substituted toluenes with the LUMO having a far greater energetic dependence on the angle of the rotor. In this way, they were able to rationalize the barriers to internal rotation in the S_1 state of a range of monosubstituted toluenes.

The bulk of both theoretical and experimental work to date has concentrated on the methyl rotor. In contrast, the CF_3 rotor has received much less attention. Hollas and co-workers,[7−10] using a variety of methods, have examined the torsional spectrum of the isomers of (trifluoromethyl)aniline (usually abbreviated to ABTF from aminobenzotrifluoride) in the S_0 and S_1 states. The barriers to internal rotation they derived display trends with electronic state and substituent position that are similar to those seen with the methyl rotor. In this paper, we extend the work of Hollas to the ionic ground state of the isomers of ABTF by using ZEKE spectroscopy in a two-color (1+1′) excitation scheme with the torsional levels of the S_1 state as resonant intermediates. If barrier heights and equilibrium configurations are largely determined by the same hyperconjugation effects that were invoked for the CH_3 rotor, then the same trends should be observed in the ABTF analogues. Substituting F for H changes the sign of the residual atomic charges in the CX_3 group, and if electrostatic effects between

† Part of the special issue "Edward W. Schlag Festschrift".
* To whom correspondence should be addressed.

10.1021/jp004001p CCC: $20.00
Published on Web 04/14/2001

the CF_3 group and the NH_2 group are dominant in the ion, new trends will emerge.

The rotor eigenstates τ belong to one of three symmetry species (six in the case of the para isomer), and this, together with the associated spin eigenstates of the three F or H atoms, gives rise to selection rules for rotor transitions accompanying the electronic transition. In the case of the methyl rotor, these rules are found to be largely, but not exclusively, followed both in the ZEKE spectrum of the D_0 (τ^+) $\leftarrow$ S_1 (τ') transition and in the torsional structure of the S_1 (τ') $\leftarrow$ S_0 (τ'') REMPI spectrum. Using the intensities of the torsional structure of the ZEKE spectra in this paper, we will explore these rules in situations where the energy separation between rotor states of different symmetry is much smaller than that encountered with the methyl rotor.

2. Experimental Section

The experimental arrangement for the ZEKE-PFI studies has been previously described[11] and only a brief outline is given here. The photoelectron spectrometer consists of a differentially pumped vacuum chamber, a pulsed nozzle source, electron/ion collection optics and a 40 cm time-of-flight tube with an MCP detector. The electron/ion current was integrated by a Stanford Research SR250 boxcar. Samples of each isomer of ABTF were used without further purification, and their vapor pressure at room temperature was high enough for sufficient to be taken up by He at 1 atm flowing over the liquid surface. The resulting mixture was expanded through a pulsed nozzle (General Valve, orifice diameter 300 μm, and then skimmed (Beam Dynamics, diameter 0.49 mm). Lower backing pressures were used to obtain spectra via hot bands. The laser system consisted of two dye lasers (Quanta-Ray PDL-2 and PDL-3) pumped by the second harmonic of a Nd:YAG laser (Quanta-Ray DCR2A). The outputs of both dye lasers were frequency doubled in KDP to produce the UV wavelengths required. The pump photon (200 μJ) was unfocused, while the probe (700 μJ) was focused with a 15 cm focal length fused silica lens. All quoted wavelengths have been corrected for vacuum and calibrated using the neon optogalvanic lines.

3. Spectra and Assignments

3.1. Symmetry and Torsional State Notation. Rotation of the CF_3 group in the 2- and 3-isomers of ABTF generates a potential that can be expanded in the form

$$V(\phi) = \frac{1}{2}\sum_{n=1} V_{3n}(1 - \cos(3n\phi)) \qquad (1)$$

where ϕ is the azimuthal angle of a chosen F atom with respect to the y/z plane that contains the benzene ring (see Figure 1). $V(\phi)$ as written in eq 1 has a minimum at $\phi = 0$ and a maximum at $\pi/3$. For 4-ABTF the expansion is in cos ($6n\phi$). $V(\phi)$ in eq 1 is unchanged under the coordinate transformations (which must be pure rotations of the rotor to be realizable) $\phi \rightarrow \phi + (2\pi/3)$, $\phi \rightarrow \phi + (4\pi/3)$, and $\phi \rightarrow -\phi$, $-\phi + (2\pi/3)$, $\phi \rightarrow -\phi + (4\pi/3)$. These two classes of operations, together with E, generate a group that is isomorphous with C_{3v} or[13] D_3 and also with the extended group G_6. Rotor eigenfunctions can thus be classified as a_1, a_2, and e. The correlation diagram for the evolution of the rotor energy levels with barrier height is shown in Figure 2. In the high barrier limit, to the right in Figure 2, states that are more than $\sim$100 cm^{-1} below the top of the barrier are effectively 3-fold degenerate, the bands comprising alternately

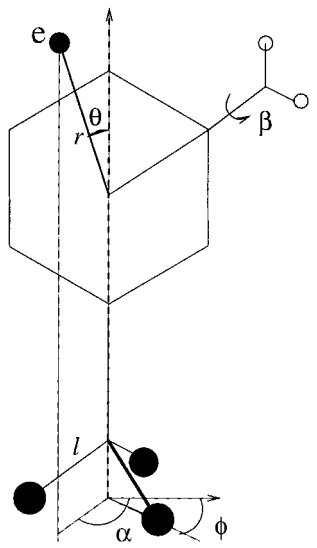

Figure 1. Coordinates for the coupling of a Rydberg electron e with the internal rotation of the CX_3 rotor (azimuthal angle ϕ) or the NH_2 group (β).

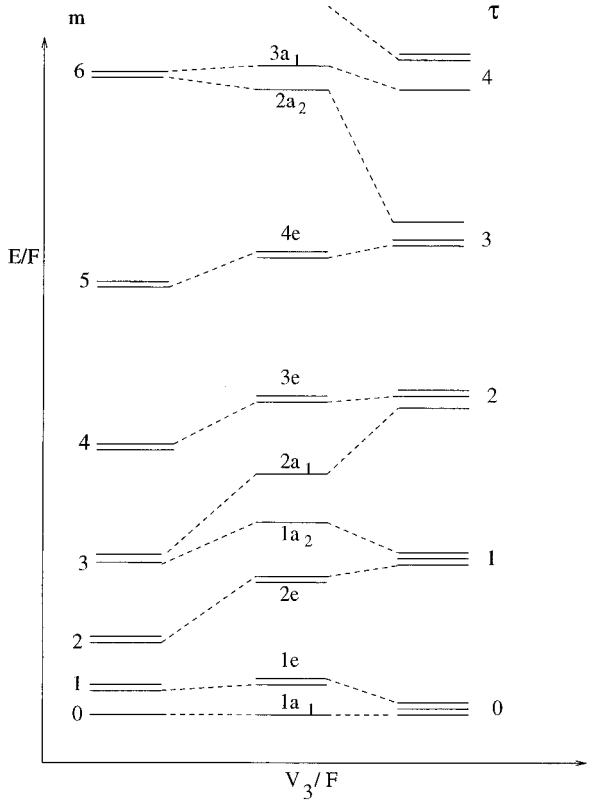

Figure 2. Correlation diagram for the reduced energy levels (E/F) of a hindered rotor with reduced barrier height for a potential of the form V_3 cos 3ϕ. The limiting case on the left, $V_3/F = 0$ corresponds to a free rotor and on the right the levels shown are below the barrier but the growing separation of the e and a levels with increasing τ is indicated. In the middle stack, the reduced barrier height V_3/F is between the energies of the $4e$ and $2a_2$ levels.

a_1, e and a_2, e levels. An important difference between the spectroscopy of the CH_3 and CF_3 rotors arises because the value of the internal rotational constant $\tilde{F}$ is $\sim$20 times greater for CH_3. Consequently, for a torsional level at a given energy below the barrier maximum, there is far less tunneling interaction between the potential wells with CF_3 and torsional levels are then best labeled with a single index τ as on the right of Figure

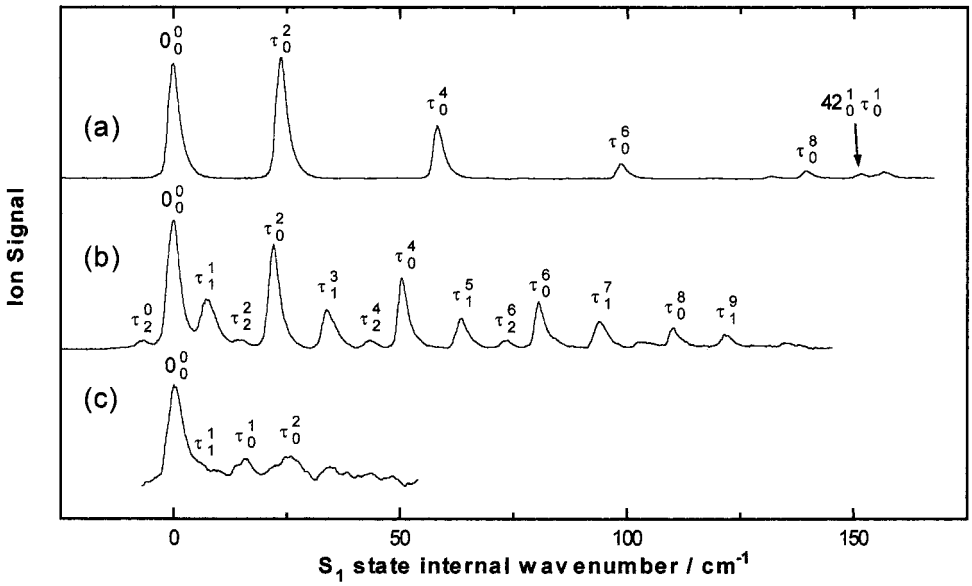

Figure 3. REMPI spectra of (a) 2-ABTF, (b) 3-ABTF, and (c) 4-ABTF, all via the S_1 resonant intermediate state.

2. Band energies well below the barrier, where the potential is nearly quadratic, are then given by

$$E_\tau \simeq \left(\tau + \frac{1}{2}\right)\sqrt{(2\tilde{F}\tilde{k})}; \quad \tilde{k} = \frac{9}{2}\sum_{n=1,2.} n^2\tilde{V}_{3n} \qquad (2)$$

In the para-isomer, $V(\phi)$ posseses the additional symmetry operations[14] (iii) $\phi \rightarrow \pi - \phi$, (iv) $\phi \rightarrow \phi - 5\pi/3$, $\phi + \pi/3$ and (v) $\phi \rightarrow \phi + \pi$, $\phi + 5\pi/3$, $\phi - \pi/3$, making the expanded group isomorphous with G_{12} or with the point groups C_{6v} and D_{3h}. In the high barrier (or isolated well) limit, the energy levels form bands that are effectively 6-fold degenerate, comprising alternately $\{a_1', e'', e', a_2''\}$ for even τ and $\{a_1'', e', e'', a_2''\}$ for odd τ. However, barriers are considerably lower in the absence of a V_3 term in the potential, and the bands, apart from the lowest, are split into doublets. The notation $0a_1'$, $1e''$, $2e'$, $3a_2''/3a_1''$, ... is then adopted, in which the index τ is now equivalent to the free rotor quantum number m which numbers successive pairs of energy levels.

If the complete wave function can be factored in the standard fashion

$$\Psi = \psi_e\psi_{v1} \ldots \psi_{v3N-5}\psi_\tau\psi_{JM} \qquad (3)$$

then, as discussed by Weisshaar,[2] the selection rule for internal rotation transitions accompanying an electronic transition is that they are symmetry-conserving, provided that the dipole operator does not depend on the coordinate ϕ. Although jet-cooling is used in the ZEKE experiments, it is difficult to collisionally induce transitions between torsional states of different symmetry even though the energy gap might be only a few cm^{-1}, and $a \leftrightarrow e$ is forbidden because of the change in spin parity that would be required. Thus in the 2- and 3-isomers there is essentially equal population of the a_1 and e states.

Furthermore, as long as the torsional wave functions $\psi_\tau(\phi)$ remain confined to the potential wells with essentially no penetration of the barriers, and if the potential functions for the initial and final electronic states (i.e. S_0/S_1 at the pump stage and S_1/D_0 at the probe stage) remain "in phase" with maxima aligned with maxima, then ee transitions between odd and even τ levels have effectively zero Franck−Condon (FC) factors inspite of being allowed by symmetry. It is only near the top of the barrier that these transitions are seen. If, on the other hand, the upper and lower potentials are out of phase, so that maxima are aligned with minima, then $e \rightarrow e$ transitions in which $\Delta\tau$ is odd may be seen strongly. Such an arrangement would of course lead to the origin band being very weak. Finally, if the intensities of lines are to be interpreted, the weighting of 2:1 for an a_1 or a_2 state relative to a single estate that arises from the spin statistics must be taken into account.

3.2. (1+1) REMPI Spectra. Figure 3 shows the (1+1) REMPI spectra of all three geometric isomers of ABTF presented relative to their S_1 origins. The spectra are essentially identical to those obtained by Hollas and co-workers[7−10] by fluorescence excitation. Each spectrum displays the effects of the selection or propensity rules outlined above. Thus, in the 2-isomer only the *even* $n \leftarrow 0$ progression is seen, pointing to (1) negligible population of the $\tau = 1$ band in the S_0 state and (2) the S_0 and S_1 potentials being in-phase. A weak combination band, $42_0^1\tau_0^1$ is also visible; ν_{42} is the NH_2 torsional mode and twisting the NH_2 group out of the plane of the benzene ring reduces the symmetry of $V(\phi)$ for the CF_3 rotor from C_{3v} to C_3 so that the distinction between a_1 anda_2 states is lost. In the 3-isomer, both *odd* ← *odd* and *even* ← *even* transitions are seen, with transitions originating from $\tau = 0$, 1, and 2 of the S_0 state being visible. The S_0 potential clearly has a very low barrier in order for three energy levels to be appreciably populated, and the absence of *odd* ↔ *even* transitions points to the S_0 and S_1 state potentials being in-phase. The potential parameters obtained by Hollas et al. for these states are listed in Table 1 for comparison with the results on the ion to be presented.

The 4-ABTF spectrum contains only a very short progression, but both $\Delta\tau = 1$ and $\Delta\tau = 0$, 2 transitions are seen. The unresolved shoulder on the origin band can be assigned as the sequence band τ_1^1, pointing to an appreciable population of $\tau = 1$ in the beam and hence to a very shallow S_0 potential. The appearance of both odd and even $\Delta\tau$ transitions might be due to the S_0 and S_1 potentials being out of phase, or to appreciable overlap of the rotor wave functions in adjacent potential wells because of the very low barrier. However, the strong origin band clearly indicates that the potentials are aligned.

3.3. (1+1′) ZEKE-PFI of 2-ABTF. The $\tau = 0$, 2, 4, 6, and 8 levels of the S_1 state of 2-ABTF were used as resonant intermediate levels in a two-color ZEKE-PFI excitation scheme.

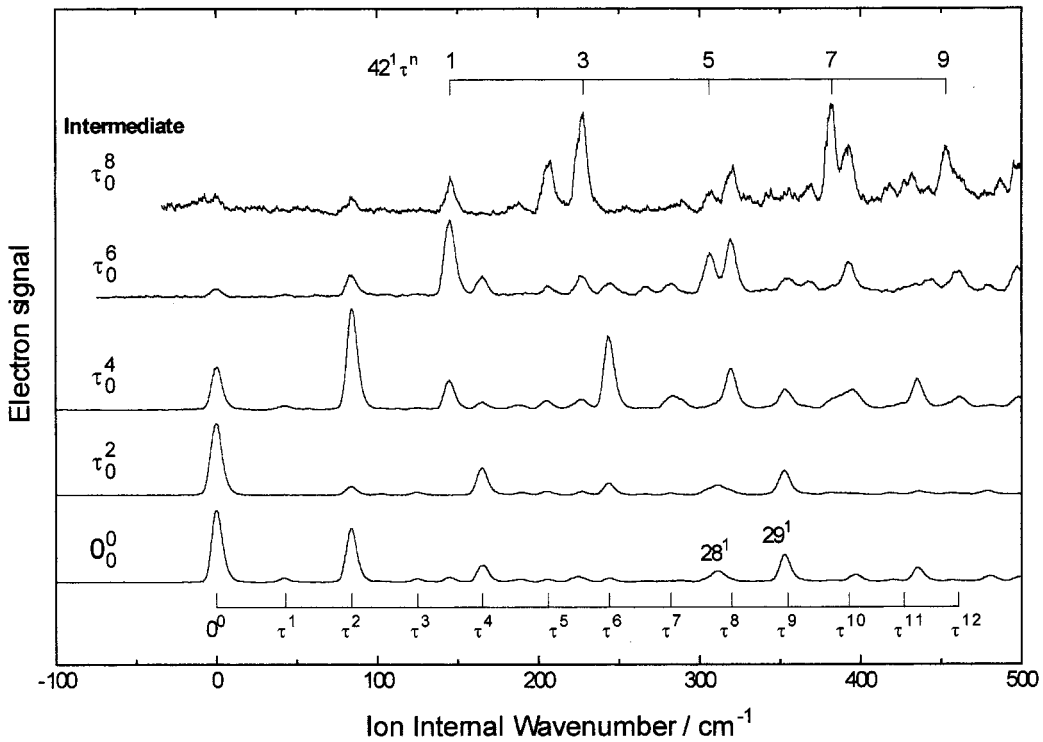

Figure 4. ZEKE spectra of 2-ABTF via even $\tau = 0-8$ of the S_1 state. The positions of the torsional levels τ^+ of the ion are indicated below the ZEKE spectrum via the origin band.

TABLE 1: Comparison of the Parameters V_3, V_6, and F for the Three Isomers of ABTF and the Corresponding Aminotoluenes (AT) in the S_0, S_1, and D_0 States

molecule	V_3/cm^{-1}	V_6/cm^{-1}	F/cm^{-1}	ref.
2-ABTF				
S_0	450	83	0.29	10
S_1	240	−67	0.29	10
D_0	720	−3	0.29	a
2-AT				
S_0	703	62	5.28	5
S_1	40	−11	5.40	5
D_0	649	19	5.20	5
3-ABTF				
S_0	9	−10	0.29	8
S_1	155	−40	0.29	8
D_0	222	−4	0.29	a
3-AT				
S_0	9	−10	5.37	5
S_1	340	−22	4.77	5
D_0	248	−13	5.20	5
4-ABTF				
S_0		5	0.38	9
S_1		33	0.38	9
D_0		12	0.32	a
4-AT				
S_0		5.6	5.473	12
S_1		44	5.408	12
D_0	–	–	–	–

[a] From this work.

These are shown in Figure 4. The torsional progression in the ion can be observed up to $\tau = 12$. The $\tau = odd$ levels are barely visible, indicating (i) no change in the positions of the potential minima for internal rotation, which would lead to the e components of $\tau \leftrightarrow \tau \pm 1$ transitions gaining intensity, and (ii) the selection rule $a_2 \not\leftrightarrow a_1$ still holds. Substantial intensity can also be seen in the NH_2 torsional mode (υ_{42}) in combination with the CF_3 torsion. These combination bands become more pronounced as the torsional level of the intermediate state increases, until at τ_0^8 they dominate the spectrum. The intensity of these lines indicates substantial coupling in the ion core between the two torsional modes, which is greater than in the S_1 state where such combination bands are largely absent.

TABLE 2: Torsional Energy Levels of [2-ABTF]$^+$, Observed and Calculated Using $V_3 = 720$ cm^{-1}, $V_6 = -3$ cm^{-1}, and $F = 0.290$ cm^{-1}

τ^+	E_{calc}/cm^{-1}	E_{obs}/cm^{-1}	τ^+	E_{calc}/cm^{-1}	E_{obs}/cm^{-1}
1	42.3	43	7	282.2	282
2	84.0	84	8	319.6	320
3	125.1	125	9	356.1	355
4	165.4	165	10	391.9	393
5	205.1	206	11	426.7	-
6	244.0	244	12	460.6	461

The field-free adiabatic ionization energy is found to be 65 373 ± 3 cm^{-1}. Torsional energy levels of the CF_3 rotor are listed in Table 2 along with those calculated using the potential parameters $V_3 = 720 \pm 10$ cm^{-1} $V_6 = -3 \pm 4$ cm^{-1}, and $F = 0.290 \pm 0.004$ cm^{-1}. The energy levels are fitted to within experimental resolution, but because they only extend to two-thirds of the barrier height, no separation of the e and a components of even the highest τ cluster is resolvable and the barrier height can only be equated to V_3 if V_9 is assumed to be zero. With this potential, and assuming the conservation of symmetry in the rotor transitions, the calculated FC factors are displayed in Figure 5. $\Delta\tau = odd$ transitions do indeed seem to be absent, but apart from this the fit of the intensities is poor even if the combination bands are neglected. The undulating profile of torsional progressions that is characteristic of Franck−Condon controlled transitions is hardly apparent, except in the spectrum originating from the pump transition τ_0^4. We return to this problem after a description of the ZEKE spectra of the other two isomers.

3.4. (1+1) ZEKE-PFI of 3-ABTF. The ZEKE-PFI spectra of 3-ABTF *via* $\tau = 0-8$ of the S_1 state are presented in Figure 6. The presence of hot bands allows odd torsional levels to be used as resonant intermediates. The origin band is absent, and

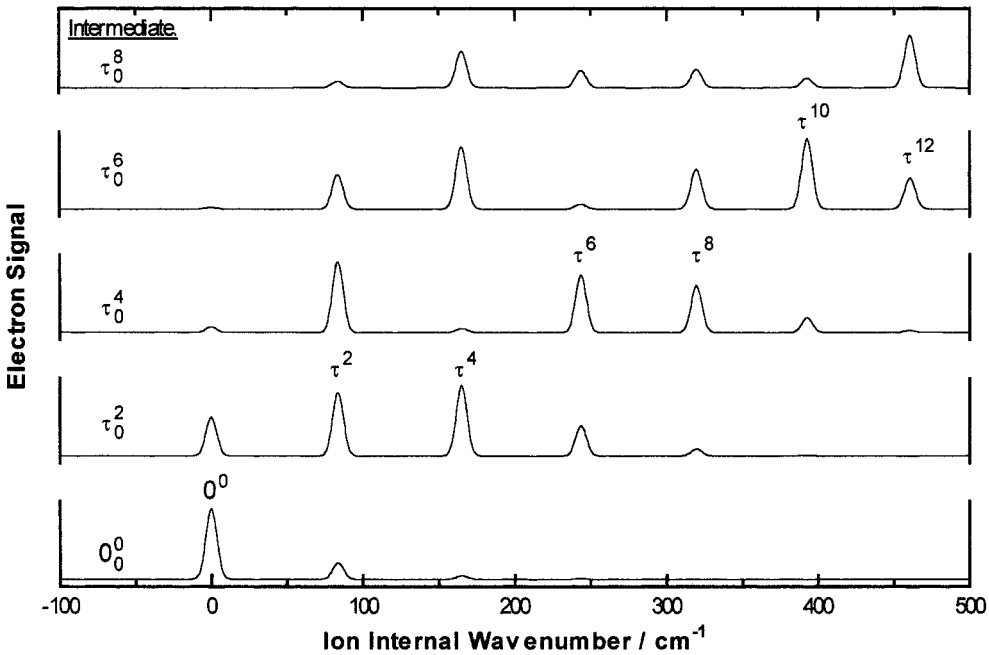

Figure 5. Simulated ZEKE spectra of 2-ABTF via even $\tau = 0-8$ of the S_1 state, using calculated Franck−Condon factors from the overlap of the wave functions of like symmetry species in S_1 and D_0.

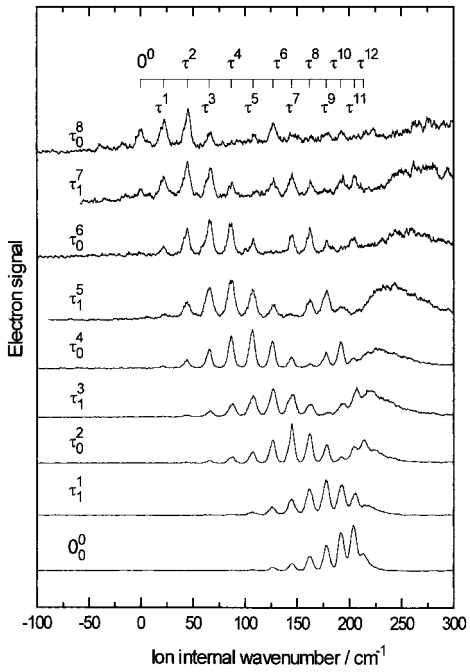

Figure 6. ZEKE spectra of 3-ABTF via $\tau = 0-8$ of the S_1 state. Torsional energy levels of the ion are indicated at the top.

we have deduced the field-free ionization energy from the longest wavelength transition in the ZEKE spectrum from the highest intermediate rotor state, giving the value of 654 503 cm^{-1}. Two considerably weaker features further to the red are assigned to transitions originating from a hot band of $S_1 \leftarrow S_0$ which partially overlaps the resonant transition. Table 3 lists the internal energies of the torsional levels along with those calculated for a potential with parameter values $V_3 = 222 \pm 10$ cm^{-1}, $V_6 = -4 \pm 2$ cm^{-1}, and $F = 0.290 \pm 0.005$ cm^{-1}. Agreement is again well within experimental resolution, and in contrast to 2-ABTF, the data points cover the entire range to the top of the barrier, whose height can be reliably equated to V_3.

TABLE 3: Torsional Energy Levels of [3-ABTF]$^+$, Observed and Calculated Using $V_3 = 222$ cm^{-1}, $V_6 = -4$ cm^{-1}, and $F = 0.290$ cm^{-1}

τ^+	E_{calc}/cm^{-1}	E_{obs}/cm^{-1}	τ^+	E_{calc}/cm^{-1}	E_{obs}/cm^{-1}
1	22.7	22	9	178.8	178
2	44.8	45	10	193.2(a_1)	192
3	66.3	66		193.6(e)	
4	87.1	87	11	206.2(a_2)	205
5	107.3	108		208.6(e)	
6	126.6	127	12	213.8(a_1)	214
7	145.1	145		217.5(e)	
8	162.6	162			

The Franck−Condon factors calculated for the D_0S_1 transition are shown in Figure 7 for the even- τ resonant intermediate states. The extent of the torsional progressions is well reproduced, but the calculated intensities show an oscillation between adjacent lines that is absent in the smooth envelope of the observed spectra. This oscillation arises because $\Delta\tau = odd$ transitions only have a contribution from the $e \rightarrow e$ component, whereas both $e \rightarrow e$ and $a_1/a_2 \rightarrow a_1/a_2$ transitions contribute to the unresolved $\Delta\tau = even$ line strengths. Since the a states have a weight equal to that of the combined e states, and in the harmonic oscillator approximation the Franck−Condon factors $\langle a,\tau'|a,\tau^+\rangle^2$ and $\langle e,\tau'|\ e,\tau^+\rangle^2$ are equal, a pronounced odd/even alternation in intensity results, as shown in Figure 7.

3.5. (1+1) ZEKE-PFI of 4-ABTF. We obtained a ZEKE spectrum via only one torsional level of the S_1 state, giving the origin band shown in Figure 8. The field-free ionization energy was found to be 65886 ± 3 cm^{-1}. A limited progression of only three torsional levels in the ion was observed, with a spacing of 7 cm^{-1}. This small amount of data can be fitted with the potential parameter values $V_6 = 12 \pm 5$ cm^{-1}, $F = 0.32 \pm 0.05$ cm^{-1}.

4. Discussion

4.1. Barriers to Internal Rotation of the CF3 Group. Potential functions $V(\phi)$ for the three isomers of ABTF are plotted in Figures 9−11, using the V_3 and V_6 coefficients listed in Table 1. The corresponding values for the aminotoluenes are

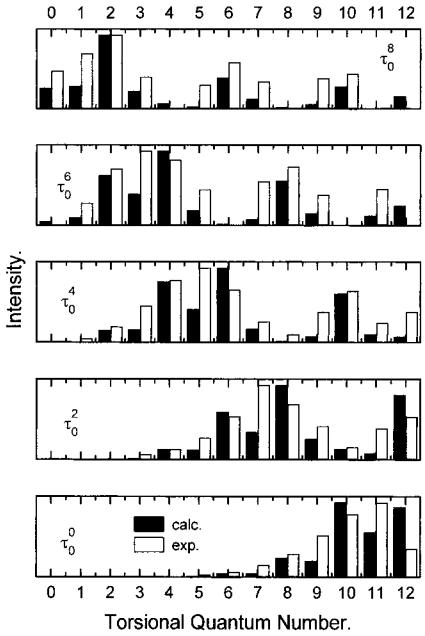

Figure 7. Observed and calculated intensities of ZEKE spectra of 3-ABTF via $\tau = 0-8$ of the S_1 state, the latter with the state with $a_1 \rightarrow a_1$ and $a_2 \rightarrow a_2$ transitions included.

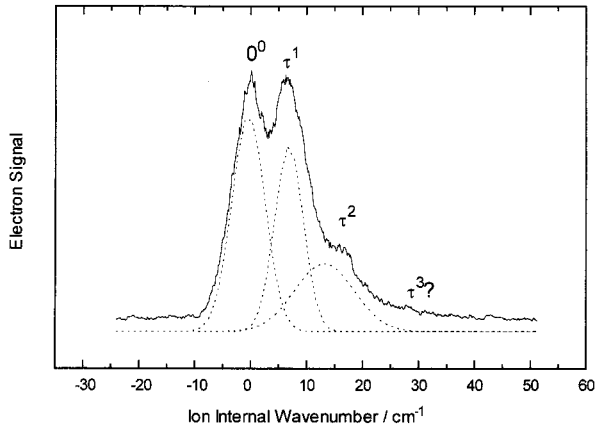

Figure 8. ZEKE spectrum of 4-ABTF.

also tabulated, and the similarity between the fluorinated and CH_3 species is clear, both in terms of the magnitude of the potential barriers and the changes in equilibrium conformation. This similarity reinforces the view that barriers to internal rotation of the CX_3 group in substituted toluenes arise principally from the interaction of the *e* orbitals of the rotor with the π-orbitals of the ring, rather than from steric/electrostatic interactions between the CX_3 and NH_2 groups. However, we will see that the CF_3–NH_2 interaction does have a marked effect on line intensities in the ZEKE spectra, even though the torsional energy levels, judged by the goodness of fit obtained by using the uncoupled rotor model, are displaced by less than ± 1 cm^{-1}.

4.2. Intensities in the ZEKE Spectra. The τ^+-progressions in the ZEKE spectra for 3-ABTF all show a slowly oscillating profile that is expected as the overlapping portions of the upper and lower state wave functions pass in and out of phase as τ^+ is scanned. This is characteristic of a Franck−Condon envelope of transitions between displaced potentials. However, when we come to simulate the band intensities using the ionic state potential obtained by fitting the line positions, an unexpected discrepancy emerges. Recalling that the symmetry of rotor states is $\{a_1,e\}$ in even numbered bands and $\{a_2,e\}$ if τ is odd, the

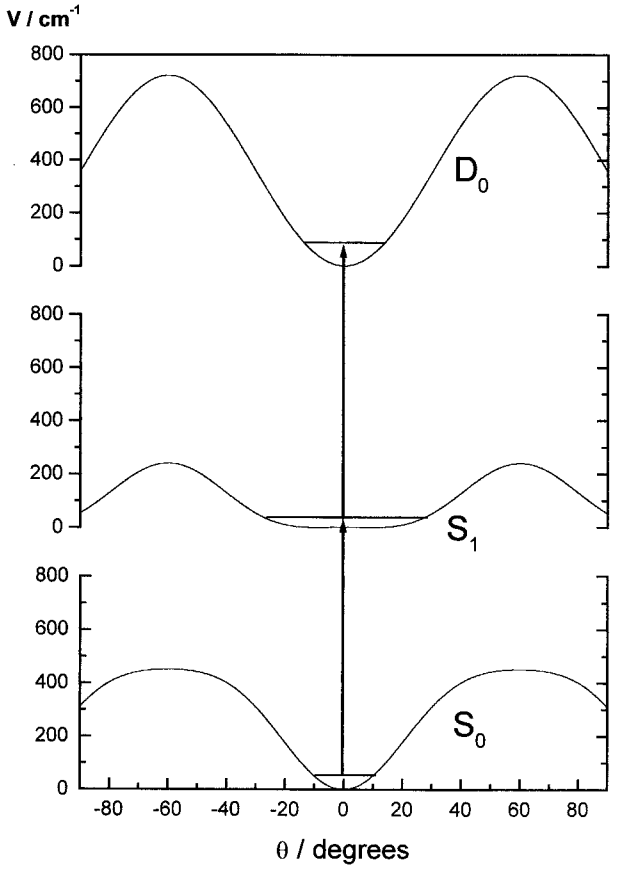

Figure 9. Potentials for internal rotation of CF_3 for the S_0, S_1, and D_0 states of 2-ABTF.

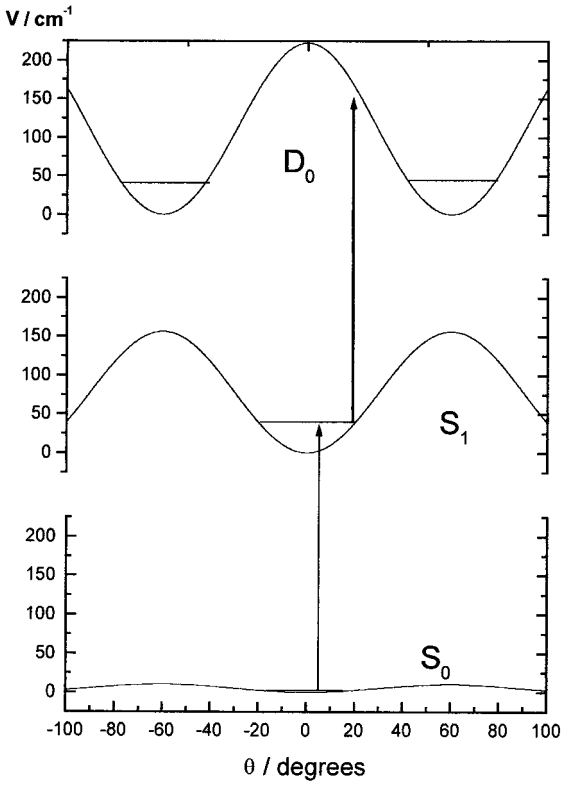

Figure 10. Potentials for internal rotation of CF_3 for the S_0, S_1, and D_0 states of 3-ABTF.

symmetry-conserving selection rule for rotor states accompanying an electronic transition predicts an alternation in intensity between the $\Delta\tau = odd$ and *even* lines in a torsional progression

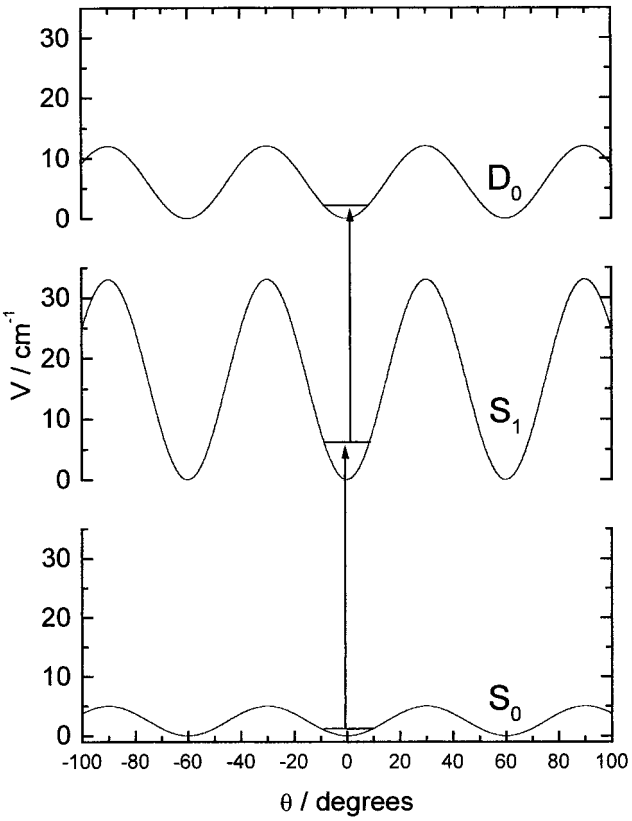

Figure 11. Potentials for internal rotation of CF_3 for the S_0, S_1, and D_0 states of 4-ABTF.

because only $e \rightarrow e$ transitions can contribute to the former, but both $a_1 \rightarrow a_1$ (or $a_2 \rightarrow a_2$) and $e \rightarrow e$ are present in the even $\Delta\tau$ transitions. Furthermore, as can be readily demonstrated by approximating the eigenfunctions with symmetry-adapted linear combinations of harmonic oscillator wave functions that are localized in each well, the *a* and *e* components of a $\Delta\tau = even$ transition have comparable Franck−Condon factors. $\Delta\tau = even$ transitions should thus have 3/2 times the intensity of $\Delta\tau =$ *odd* ones. However, the envelope of the torsional progression in the ZEKE spectrum of the 3-isomer does not show any odd/even alternation, only the slower FC oscillation spanning several torsional levels. The point is made in Figure 12, where we have plotted the intensities calculated assuming only $e \rightarrow e$ transitions and in Figure 7 where the $a_1 \rightarrow a_1$ and $a_2 \rightarrow a_2$ transitions, weighted equally to the *e* transitions, have been included, but not the forbidden $a_1 \leftrightarrow a_2$ ones. Either only *e* states are present or the $a_1 \not\leftrightarrow a_2$ restriction is completely relaxed, which would restore the smoothness of the envelope.

There is no reason to suppose that the a_1 species is absent from the parent beam, where the $0a_1$ and $1e$ states are essentially degenerate in the $\tau = 0$ band, and both would be pumped to the S_1 electronic state within the bandwidth of the laser. $a_2 \leftrightarrow a_1$ transitions are seen weakly in both the 2- and 3-isomers of fluorotoluene[15] and in 3-toluidine where they have ∼10% of the intensity of allowed transitions. Thus the behavior of the CF_3 rotor in this respect represents the evolution of a trend that is already apparent in the CH_3 rotor. The $a_1 \not\leftrightarrow a_2$ restriction would be lifted if the two species were mixed by rotor/electronic interaction. This could occur in either the S_1 state or close to the ionization limit after the probe step. There is no evidence for $\Delta\tau =$ odd transitions in the $S_1 \leftarrow S_0$ REMPI spectrum (Figure 3), so the mixing of a_1 and a_2 states must occur after the probe step. Takazawa et al.,[15] discussing the much weaker

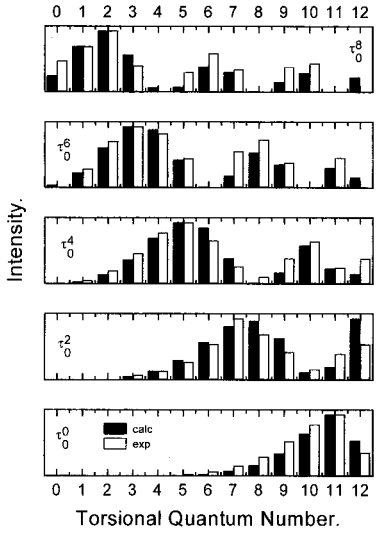

Figure 12. Intensities of ZEKE spectra of 3-ABTF, observed and calculated assuming only $e \rightarrow e$ transitions.

and more sporadic forbidden bands in the fluorotoluenes, reached the same conclusion and also gave reasons for rejecting coupling with the overall rotation as an explanation. Their favored mechanism is the same one that is responsible for non-Franck−Condon intensities observed in the vibrational ZEKE spectroscopy of diatomic molecules,[16] and we now show why Rydberg−rotor coupling near an ionization threshold might become a facile process for heavy rotors. Each rotor state τ^+ of the ion has a Rydberg progression associated with it that passes through the ionization thresholds of all the lower τ^+ states. ZEKE spectroscopy probes a narrow energy band extending ∼6 cm^{-1} below each ionization threshold. Rydberg states based on higher τ^+ levels that fall within these energy bands can act as doorway states in the creation of long-lived ZEKE states. We now need to find the probability of such Rydberg states lying within the ZEKE energy bands and if there is a term in the electron−core potential that can couple a_2 and a_1 states. Even if these conditions are fulfilled, it must be remembered that this vibronic coupling is unusual in that the already high electronic energy is increased and the vibrational energy lowered, the reverse of the usual direction of internal conversion.

In 3-ABTF, adjacent rotor states in the ion are separated by ∼22 cm^{-1} near $\tau = 0$ and ∼13 cm^{-1} near the top of the barrier at $\tau = 10$, 11. The density of Rydberg states 22 cm^{-1} below the ionization limit of a given τ^+ level (corresponding to $n \sim 70$) is $dn/dE = 1.6/cm^{-1}$, and $3.5/cm^{-1}$ for rotor levels just below the barrier ($n \sim 90$). Thus between at least 10 and 30 Rydberg states converging on the next highest torsional level lie in the energy band of each torsional level probed by ZEKE spectroscopy. This number will increase if more than one series (*ns*, *np*, etc) can be accessed from the S_1 intermediate state. Because of the continuity of the ionization/excitation cross section across an ionization limit, the integrated absorption cross section, taken over the laser bandwidth, for exciting the high-*n* Rydberg states based on the τ^+ core state is equal to that for exciting the coincident lower *n* states based on $\tau^+ + 1$. In other words, exactly the same size of ZEKE signal would be observed via excitation directly to states with $n \sim 100$ based on a given τ^+ state as via the band of lower *n* states based on $\tau^+ + 1$, assuming equal conversion probability to ZEKE states. Adjacent torsional states of the CH_3 rotor in, say, 2-fluorotoluene[15] are separated by 100 cm^{-1}, corresponding to a density of states ≈ 0.16/ cm^{-1}, so an average of one Rydberg state will lie in the

ZEKE bandwidth. This is still sufficient to produce a marked enhancement of the ZEKE signal. However, in general $a_2 \leftrightarrow a_1$ transitions in the ZEKE spectrum of 2- and 3-fluorotoluene are observed[15] to be weak or absent, even when the energy gap between adjacent a_2 and a_1 states becomes smaller above the barrier in the ion. We thus need an additional factor to explain the facile $a_2 \leftrightarrow a_1$ transitions of the CF_3 rotor accompanying threshold ionization.

The form of the coupling term between a Rydberg electron and the F atoms of the rotor can be quickly deduced with the aid of Figure 1. The origin of the polar coordinates (r,θ,ϕ) of the electron is at the center of the benzene ring, which lies in the *x*/*y* plane. The azimuthal angle of the rotor with respect to this plane is α, and the displacement of the centroid of the three F atoms along the *z*-axis is *d*. The interaction between the electron and the residual charges *q* on the F atoms can only depend on the difference in azimuthal angles $(\alpha - \phi)$ and must be unchanged under the transformation $\phi \rightarrow \phi + n\pi/3$, or the equivalent change of α. The leading term in $V_e(r,\theta,\phi,\alpha)$ must thus be cos $3(\phi - \alpha)$. In the limit $r \gg d, l$ the result is

$$V_e(r,\theta.\phi,\alpha) = \frac{15}{16}\frac{eql^3}{r^4}\sin^3\theta\cos 3(\phi - \alpha) \qquad (4)$$

where *q* is the residual charge on the F atom and *l* is the radial distance of the F atoms from the *z*-axis (in this multipolar expansion this is the leading charge−octupole interaction). In terms of spherical harmonics of the polar coordinates,

$$V_e(r,\theta.\phi,\alpha) = \frac{15e\Omega}{16r^4}\sin 3\alpha\{C_{33}(\theta,\phi) + C_{3-3}(\theta,\phi)\} + \cos 3\alpha\{C_{33}(\theta,\phi) - C_{3-3}(\theta,\phi)\} \quad (5)$$

where Ω is the octupole moment of the rotor, ql^3. The term in sin 3α has a_2 symmetry in the C_{3v} group applied to the rotor alone and the cos 3α term is a_1. The sin 3α term can thus induce $a_2 \leftrightarrow a_1$ transitions, *i.e* $\Delta\tau^+ = odd$, and the cos 3α term $\Delta\tau = even$. These will be partnered by $\Delta l = \pm 1, \pm 3$, $\Delta m_l = \pm 3$ transitions of the Rydberg electron, thus coupling the *s* with the *f* series and the *d* with the *p* or *f* series. We deduce from the fact that $a_2 \leftrightarrow a_1$ transitions appear to be fully allowed that the internal conversion, $\Delta\tau^+ = -1$, $\Delta n \lesssim +50$, is rapid compared with the radiative lifetimes of the doorway states, or with competing internal conversion channels involving other vibrational modes.

However, we still have to explain why $a_2 \leftrightarrow a_1$ transitions are very weak in the ortho isomer, where the separation of adjacent torsional levels is ∼40 cm^{-1}. This corresponds to a density of Rydberg states of ∼0.6 cm^{-1} which is still enough to allow three or four such autoionizing states to lie within the ZEKE bandwidth. The explanation of the dependence of forbidden torsional transitions on the position of substitution of the rotor on the ring might be sought in two directions. First, the r^{-4} dependence of the Rydberg electron−rotor interaction in eq 4 means that the major contribution to the vibronic coupling matrix element $\langle\tau^+, n_1|V_e|\tau^+ - 1, n_2\rangle$ comes from the inner lobes of the electronic wave function. This part of a Rydberg wave function is very sensitive to the location of the valence orbitals to which it must remain orthogonal. The NH_2 group interacts strongly with the ring π-electrons and the electron density at the ortho and meta positions is different, leading to a different probability distribution of the Rydberg electron in the vicinity of the rotor, and hence to a different strength of vibronic coupling. Perhaps a more probable explanation of the change in propensity for forbidden $a_2 \leftrightarrow a_1$ transitions of the rotor with its position in the ring is suggested by the observation in the ortho isomer of much stronger combination bands involving the CF_3 torsional mode and the NH_2 twisting mode.

4.3. Combination Bands Involving CF_3 and NH_2. The NH_2 twisting mode, ν_{42}, is governed by a double minimum potential of the form $V(\beta) = V_2 \cos 2\beta$, where β is the dihedral angle between the NH_2 plane (effectively planar because of the rapid inversion) and the plane of the benzene ring (see Figure 1). The symmetry operations of the local environment for this internal rotation generate a group isomorphous with C_{2v} and energy levels below the barrier between the two minima are effectively pairwise degenerate, alternating in symmetry species $\{a_1, b_1\}$ for $\nu_{42} = even$ and $\{a_2, b_2\}$ for $\nu_{42} = odd$. Transitions in this mode are thus restricted to $\Delta v = even$ and in particular 42_0^1 is missing. The progression in ν_{42} in the ZEKE spectrum of 2-ABTF excited via τ_0^8 (Figure 4) is thus assigned to $42_0^1\tau_0^n$, n *odd*. This progression is absent in the 3-isomer. The REMPI spectrum of 2-ABTF shows one weak combination band $42_0^1\tau_0^1$, which is 12 cm^{-1} away from the nearest *even* τ torsional transition, τ_0^8, and no such combination band is observed in the 3-isomer. Thus in 2-ABTF the levels $42^0\tau^8$ and $42^1\tau^1$ of the S_1 state will mix to some extent and pumping τ_0^8 of $S_1 \leftarrow S_0$ will provide some Franck−Condon overlap at the probe stage with the combination state $42_0^1\tau_0^{odd}$ in the ion. Such a route is not available to the 3-isomer where there is no coupling between the CF_3 and NH_2 rotors. Equally, this coupling will occur in the ion where, for instance, the levels $42^1\tau^1$ and τ^4 are 20 cm^{-1} apart.

The effect of coupling between the CF_3 and NH_2 torsions on intensities in ZEKE spectra could arise as follows. The Rydberg electron can readily coupled with the NH_2 torsion both because of the polarity of the N−H bonds and because the leading coupling term in a multipole expansion is now the shorter range charge−quadrupole interaction rather than the charge−octupole for the CF_3 rotor. The interaction will depend on the relative azimuthal angles β of NH_2 and φ of the electron. An analysis along the lines that led to eq 5 shows that the leading term has an angular dependence of the form cos $2(\phi - \beta)$, so both $\Delta\nu_{42} = odd$ and *even* transitions can be induced. A Rydberg electron that could have been raised to a ZEKE state by a $\Delta\tau = -1$ transition of the CF_3 rotor can now rapidly lose electronic energy in exciting the 42_0^1 transition and the forbidden ZEKE channel is then lost. However, this transition is also open to the 3-isomer, and it is here that the combination bands come into play by aiding this competing internal conversion. The vibrational spacing in ν_{42} is 110 cm^{-1} in the ion and if a Rydberg electron that could have coupled with a ZEKE state by a $\Delta\tau^+ = -1$ transition induces the 42_0^1 transition instead, its principal quantum number will change from ∼40−50 to ∼20. However, this requires a near resonant energy matching of ∼5 cm^{-1} between initial and final states for efficient coupling. The spacing between Rydberg states around $n = 20$ is ∼25 cm^{-1} and such resonances might occur, but only at random. The chances are much increased if the NH_2 mode is strongly coupled to the lower frequency CF_3 torsion, which opens up a whole range of combination transitions that are very weak in the 3-isomer.

The ZEKE states themselves (or, rather, their low-*l* precursors) are also open to the same destruction by internal conversion, but a ZEKE spectrum is observed for the 2-isomer. Transition matrix elements between two Rydberg states n_1 and n_2 are proportional to $n_1^{2/3}n_2^{2/3}$, so a state 4−6 cm^{-1} below an IP

with $n \sim 100-150$ is quenched more than eight times more slowly than a state with $n \sim 50$ lying $\sim$40 cm^{-1} below. This seems to be sufficient for some pre-ZEKE states of the 2-isomer to survive long enough to be converted to high l ZEKE states.

5. Conclusions

The internal rotation of the CF_3 group in the ionic ground state of the three isomers of (trifluoromethyl)aniline has been studied using ZEKE-PFI photoelectron spectroscopy. Barriers to internal rotation were obtained from a one-dimensional fit to the observed torsional energy levels. In all cases barriers were found that mirror the trends observed when the CF_3 group is replaced by CH_3. However, greater interaction with the NH_2 group was apparent with CF_3, where combination bands with the torsional mode of the amino group were seen in the ZEKE spectrum of the 2- but not the 3-isomer.

A much more striking difference between the ZEKE spectroscopy of the CF_3 and CH_3 rotors is the complete breakdown in the 3-ABTF of the selection rule that prohibits transitions between rotor states of a_2 and a_1 symmetry. We attribute this to facile internal conversion between adjacent rotor states ($\Delta\tau^+ = -1$) and high Rydberg electronic states ($\Delta n \sim +50$). This is more favored with CF_3 as the rotor than with CH_3 both because of the much closer spacing of rotor levels and the larger multipole moment of CF_3. The absence of forbidden $a_2 \leftrightarrow a_1$ transitions in the threshold ionization of the 2-isomer, where the density of Rydberg states that can enable the breakdown of the selection rule is still high, might be the result of more efficient quenching of these Rydberg states by excitation of other low vibrational modes of the molelcule. Combination bands involving the torsional modes of the NH_2 group and the CF_3 group are prominent in the ZEKE spectrum of the 2-isomer but not in the 3-isomer and probably play a key role in this internal conversion.

Acknowledgment. We are grateful to Dr. Trevor Ridley of the Laser Spectroscopy Group at Edinburgh University for detailed discussions of several aspects of this paper. N.A.McL. thanks the EPSRC for the award of a research studentship.

References and Notes

(1) *High-Resolution Laser Photoionisation and Photoelectron Studies*; Powis, I., Baer, T., Ng, C. Y., Eds,; John Wiley & Sons: Chichester, U.K., 1995.
(2) Lu, K.-T.; Weinhold, F.; Weisshaar, J. C. *J. Chem. Phys.* **1995**, *102*, 6787.
(3) Lu, K.-T.; Eiden, G. C.; Weisshaar, J. C. *J. Phys. Chem.* **1992**, *96*, 9742.
(4) Breen, P. J.; Warren, J. A.; Bernstein, E. R.; Seeman, J. I. *J. Chem. Phys.* **1987**, *87*, 1917.
(5) Ikoma, H.; Takazawa, K.; Emura, Y.; Ikeda, A.; Abe, Haruo, Hayashi, H.; Fujii, M. *J. Chem. Phys.* **1996**, *105*, 10201.
(6) Nakai H.; Kawai, M. *J. Chem. Phys.* **2000**, *113*, 2168.
(7) Gordon, R. D.; Hollas, J. M.; Ribeiro-Claro, P. J. A.; Teixeira-Dias, J. J. C. *Chem. Phys. Lett.* **1993**, *211*, 392.
(8) Gordon, R. D.; Hollas, J. M.; Ribeiro-Claro, P. J. A.; Teixeira-Dias, J. J. C. *Chem. Phys. Lett.* **1991**, *183*, 377.
(9) Gordon, R. D.; Hollas, J. M.; Ribeiro-Claro, P. J. A.; Teixeira-Dias, J. J. C. *Chem. Phys. Lett.* **1993**, *182*, 649.
(10) Ribeiro-Claro, P. J. A.; Teixeira-Dias, J. J. C.; Gordon, R. D.; Hollas, J. M. *J. Mol. Spectrosc.* **1993**, *162*, 426.
(11) Cockett, M. C. R.; Donovan, R. J.; Lawley, K. P. *J. Chem. Phys.* **1996**, *105*, 3347.
(12) Yan, S.; Spangler, L. H. *J. Chem. Phys.* **1992**, *96*, 4106.
(13) Stolwijk V. M.; Van Eijck, B. P. *J. Mol. Struct.* **1998**, *190*, 409.
(14) Lawley, K. P. *J. Mol. Spectrosc.* **1997**, *183*, 25.
(15) Takazawa, K.; Fujii M.; Ito, M. *J. Chem. Phys.* **1993**, *99*, 3205.
(16) Nemeth, G. I.; Ungar, H.; Yeretzian, C.; Selzle, H. L.; Schlag, E. W. *Chem. Phys. Lett.* **1994**, *228*, 1.